

## Arabinose is metabolized via a phosphoketolase pathway in *Clostridium acetobutylicum* ATCC 824

M. D. Servinsky · K. L. Germane · S. Liu ·  
J. T. Kiel · A. M. Clark · J. Shankar ·  
C. J. Sund

Received: 6 April 2012 / Accepted: 1 August 2012 / Published online: 25 August 2012  
© Springer-Verlag (outside the USA) 2012

**Abstract** In this report, a novel zymogram assay and coupled phosphoketolase assay were employed to demonstrate that *Clostridium acetobutylicum* gene CAC1343 encodes a bi-functional xylulose-5-P/fructose-6-P phosphoketolase (XFP). The specific activity of purified recombinant XFP was 6.9 U/mg on xylulose-5-P and 21 U/mg on fructose-6-P, while the specific activity of XFP in concentrated *C. acetobutylicum* whole-cell extract was 0.094 and 0.52 U/mg, respectively. Analysis of crude cell extracts indicated that XFP activity was present in cells grown on arabinose but not glucose and quantitative PCR was used to show that CAC1343 mRNA expression was induced 185-fold during growth on arabinose when compared to growth on glucose. HPLC analysis of metabolites revealed that during growth on xylose and glucose more butyrate than acetate was formed with final acetate:butyrate ratios of 0.72 and 0.83, respectively. Growth on arabinose caused a metabolic shift to more oxidized products with a final acetate:butyrate ratio of 1.95. The shift towards more oxidized products is consistent with the presence of an XFP, suggesting that arabinose is metabolized via a phosphoketolase pathway while xylose is probably metabolized via the pentose phosphate pathway.

### Introduction

The imminent depletion of oil reserves has revived interest in alternative liquid fuels that are compatible with current engines and distribution infrastructure. One promising gasoline alternative is butanol, which has a similar energy density to gasoline. It is less hydroscopic than ethanol and is compatible with existing automobile engines and distribution systems [16]. In the early part of the 20th century, the primary source of butanol was from acetone/butanol/ethanol (ABE) fermentation of starches by the Gram-positive, spore-forming, anaerobe *Clostridium acetobutylicum* [8, 13]. Butanol production by *C. acetobutylicum* is desirable due to its ability to metabolize a wide variety of carbohydrates found in biomass [9, 23]. As a result, the metabolism of *C. acetobutylicum* has been the subject of extensive studies and modeling efforts as researchers search for ways to increase butanol yields and use easily obtained, renewable feedstocks such as plant waste [9, 11–13, 22, 26].

Xylose and arabinose are the predominant pentoses found in plant-derived biomass and their metabolism will contribute to overall butanol yields [1, 9]. Both of these sugars are fermented by *C. acetobutylicum* and the traditional view of clostridial metabolism indicates that they are both processed via the pentose phosphate pathway (PPP) [4, 8, 9, 17]. Interestingly, there is a great disparity in the growth rates of the organism when fed arabinose or xylose with doubling times of 78 and 287 min, respectively [23]. Attempts to identify the physiological reason behind the difference in growth rate have led to the assumptions that, during growth on xylose, *C. acetobutylicum* does not efficiently transport xylose or produce enough transaldolase to rapidly process sugars via the PPP [7, 26].

**Electronic supplementary material** The online version of this article (doi:10.1007/s10295-012-1186-x) contains supplementary material, which is available to authorized users.

M. D. Servinsky · K. L. Germane · S. Liu ·  
J. T. Kiel · A. M. Clark · J. Shankar · C. J. Sund (✉)  
Sensors and Electron Devices Directorate, US Army Research  
Laboratory, 2800 Powder Mill Road, Adelphi, MD 20783, USA  
e-mail: christian.j.sund.civ@mail.mil

In a recent genome-wide transcriptomic analysis of *C. acetobutylicum* during acidogenic growth, the mRNA for a putative phosphoketolase gene, CAC1343, was expressed 6.7 fold higher in arabinose-grown cells than in xylose-grown cells [23]. In contrast, expression levels for genes encoding the PPP (transketolase, transaldolase, and epimerase) were similar during growth on both substrates, suggesting that the putative phosphoketolase encoded by CAC1343 could be responsible for the disparity in growth rates on arabinose and xylose. More recent studies confirmed that CAC1343 is induced by arabinose (but not xylose) and showed that its expression is controlled by the arabinose regulator AraR [6, 27]. Phosphoketolases are responsible for two phosphoroclastic reactions: (1) conversion of fructose-6-P (F6P) and inorganic phosphate into erythrose-4-P and acetyl-P, (2) conversion of xylulose-5-P (X5P), and inorganic phosphate into glyceraldehyde-3-P (G3P) and acetyl-P [10, 15, 21]. Mono-functional phosphoketolases acting on either F6P or X5P and bi-functional F6P/X5P phosphoketolases have been identified in a variety of organisms and are commonly associated with *Bifidobacteria* and heterofermentative lactic acid bacteria [15, 21].

Expression of a putative phosphoketolase gene by *C. acetobutylicum* during acidogenic growth on arabinose suggests the organism could use a phosphoketolase pathway PKP as well as the PPP for arabinose metabolism. Phosphoketolases are not typically associated with clostridia but a recent phylogenetic analysis of phosphoketolase genes indicated that they have been disseminated across taxa via horizontal gene-transfer events and in the *Clostridiales* order 2 of the 20 genomes screened contained putative phosphoketolase genes [21]. One of these genes was CAC1343 from *C. acetobutylicum* ATCC 824, which is the subject of the current study. In this report, we demonstrate that CAC1343 encodes a bi-functional phosphoketolase and present physiological evidence supporting our hypothesis that *C. acetobutylicum* uses a PKP during acidogenic growth on arabinose but not xylose.

## Materials and methods

### Bacterial strains and growth conditions

*Clostridium acetobutylicum* ATCC 824 was obtained from ATCC and propagated in clostridial growth media (CGM) as previously described [23]. Each liter of CGM contained:  $\text{KH}_2\text{PO}_4$ , 0.75 g;  $\text{K}_2\text{HPO}_4$ , 0.75 g;  $\text{MgSO}_4 \cdot \text{H}_2\text{O}$ , 0.4 g;  $\text{MnSO}_4 \cdot \text{H}_2\text{O}$ , 0.01 g;  $\text{FeSO}_4 \cdot 7 \text{H}_2\text{O}$ , 0.01 g; NaCl, 1.0 g; asparagine, 2.0 g; yeast extract, 5.0 g;  $(\text{NH}_4)_2\text{SO}_4$ , 2.0 g; carbohydrate, 5 g [25]. Glucose was used as the carbohydrate for routine growth. *Escherichia coli* Novablue (Novagen) was used for cloning pTXB1CAC1343 notag and pTXB1CAC1343chitin. *E. coli* BL21 cells (Novagen) were used for IPTG-induced expression of CAC1343. All *E. coli* strains were grown on Miller Luria Broth (Sigma) containing 100  $\mu\text{g}/\text{ml}$  ampicillin unless stated otherwise.

### Microarray data

Relative expression levels for CAC1343 during growth on xylose and arabinose were obtained from a previous study and are freely available in the Gene Expression Omnibus Database (accession number GSE18471) [2, 23].

### Quantitative PCR

Total RNA was isolated from exponentially growing cells, in the acidogenic phase of growth, cultured on CGM containing either 0.5 % glucose, arabinose or xylose using a Qiagen RNeasy Mini Kit (Qiagen) as previously described [23]. Genomic DNA was removed by treatment with a TURBO DNA-free kit (Ambion) using the rigorous protocol provided by the manufacturer. Removal of genomic DNA was confirmed by real-time PCR using primers for 16S DNA. RNA was converted to cDNA with a Superscript II kit (Invitrogen) according to the manufacturer's instructions. Primers for quantitative real-time PCR were generated for CAC1343 and 16S DNA using Primer3 and

**Table 1** Primers used in this study

| Primer name        | Sequence   | Use     |
|--------------------|--|---------|
| CAC1343RTsense     | CCGGTTCAATAAATGAAGG  | qPCR    |
| CAC1343RTantisense | CTGTTTCTGCCTCTCCGCTCT  | qPCR    |
| CAC16SaRTsense     | GTGGGGAGCAAACAGGATTA   | qPCR    |
| CAC16SaRTantisense | TGTTAACTGCGGCACAGAAG   | qPCR    |
| CAC1343pTXBnotagFW | ATGCAAAGTATAATAGGAAAAC   | Cloning |
| CAC1343pTXBnotagRV | CTAATACTCGAGTTATACATGCCACTGCCAATTAG                              | Cloning |
| CAC1343nostopF     | GCCAGAAATAACTAATGGCAGTGGCATGTATGCATCACGGCAGATGCACTAGTTGC         | Cloning |
| CAC1343nostopR     | GGCAACTAGTGCATCTGCCGTGATGCATACATGCCACTGCCAATTAGTTATAGTTATTTCTGGC | Cloning |

are listed in Table 1 [20]. CAC1343 was amplified in a Smart Cycler 2 (Cepheid) using the following parameters: 95 °C for 3 min, and then 95 °C 10 s, 54 °C 15 s, 72 °C 15 s (45 cycles). Fluorescence data were collected during the extension step and a melting curve was performed to confirm that only one product was formed. Amplification of 16S cDNA was performed with the same cycling parameters with an annealing temperature of 53 °C. Each reaction contained 12.5 µl of iQ SYBR Green Supermix (Bio-Rad), 200 nM of forward primer, 200 nM of reverse primer, 1 µl template, and water for a final reaction volume to 25 µl. PCR efficiencies for each primer set were calculated using LinRegPCR and relative quantification of CAC1343 was performed using the Pfaffl method using 16S RNA as the control [18, 19, 23].

#### Plasmid construction

The expression plasmid pTXB1 (New England Biolabs) was digested with NdeI and the resulting overhangs were filled in using DNA Polymerase I, Large (Klenow) Fragment (New England Biolabs). The NdeI digested blunt-ended pTXB1 was then digested with XhoI. CAC1343 was PCR amplified with Pfu polymerase (Promega) from *C. acetobutylicum* genomic DNA using primers CAC1343pTXBnotagFW and CAC1343pTXBnotagRV, which introduced a XhoI site. The blunt-ended PCR product was digested with XhoI and ligated into pTXB1 (New England Biolabs) digested as described above to form pTXB1CAC1343notag. *E. coli* Novablue cells were transformed with the pTXB1CAC1343notag ligation mixture. Ampicillin-resistant clones were sequenced to verify the presence and sequence accuracy of CAC1343. A chitin-binding domain tagged version of CAC1343 in pTXB1 was created using primers CAC1343nostopF and CAC1343nostopR to loop out the stop codon and two linker amino acids in pTXB1CAC1343notag via the QuikChange protocol (Stratagene) forming pTXB1CAC1343chitin.

#### CAC1343 expression and purification

One liter of Miller Luria Broth (Sigma) with 50 µg/ml of ampicillin was inoculated with a 10-ml overnight culture of *E. coli* BL21 DE3 containing pTXB1CAC1343chitin and grown to an  $A_{600}$  of ~0.6 at 37 °C. The culture was then moved to 21 °C, induced with 1 mM of Isopropyl  $\beta$ -D-1-thiogalactopyranoside (IPTG) overnight and then pelleted by centrifugation (4,500 rpm in a PTI F9S-4x 1000y rotor).

The *E. coli* BL21 DE3 pellet containing pTXB1CAC1343chitin was re-suspended in 20 ml of 20 mM Tris–HCl (pH 8.0), 200 mM NaCl, 1 mM EDTA, 200 µl protease inhibitor cocktail (Sigma-Aldrich) and 0.1 % triton-x-100 (Sigma). The suspension was passed through an M-110P microfluidizer (Microfluidics) to lyse the cells.

The lysate was clarified by centrifugation ( $29,000 \times g$  for 20 min) and subsequently incubated with 10 ml of chitin IMPACT beads (NEB) for 1.5 h. The protein-bound beads were then washed with 20 ml of 20 mM Tris–HCl (pH 8.0), 500 mM NaCl, 1 mM EDTA, and 0.1 % triton-x-100. The protein was removed from the beads via self-cleavage from the chitin tag by incubating the beads with 40 ml of elution buffer (20 mM Tris–HCl (pH 8.0) and 50 mM DTT). The protein solution was concentrated and then dialyzed into PBS for enzyme assays.

#### Whole-cell extract preparation

Cultures of *C. acetobutylicum* were grown in a four-vessel Das Gip bioreactor that measured the  $A_{600}$  every 30 s with a Das Gip OD probe (path length 10 mm). The temperature was maintained at 37 °C and the cultures were agitated with a Rushton impeller at 400 RPM. The 1,500-ml vessels contained 750 ml of CGM supplemented with 0.5 % of glucose or arabinose. Cultures were removed from the vessels when the  $A_{600}$  reached 0.08 and cells were isolated by centrifugation ( $7,500 \times g$  for 10 min). The cell pellets were lysed with Cellytic B+ (Sigma-Aldrich) and incubated on a shaker at 37 °C for 15 min. After lysis, the extracts were clarified by centrifugation at  $1,900 \times g$  (15 min) and dialyzed against a buffer composed of 100 mM of sodium phosphate, 30 mM of NaCl, 0.1 mM of EDTA, 1 mM of MgCl<sub>2</sub>, 2 mM of 1,4-dithio-DL-threitol and 4 ml of protease inhibitor cocktail at pH 7. The whole-cell extracts were concentrated for use in the phosphoketolase assay by membrane filtration (Amicon Ultra-30, 10,000 Da; Millipore).

#### Phosphoketolase activity assay

Phosphoketolase activity was determined by acetyl-P production using the Racker procedure as modified by Meile et al. [5, 15]. The assay converts acetyl-P to ferric acetyl hydroxamate, which is quantified using a spectrophotometer. Each well of a 96-well plate contained 75 µl of 33.3 mM potassium phosphate (pH 6.5), L-cysteine hydrochloride (1.9 mM), sodium fluoride (23 mM), sodium iodoacetate (8 mM), thiamine pyrophosphate (1 mM), either fructose 6-phosphate (27 mM) or xylulose 5-phosphate (27 mM) (Sigma) [15]. The reaction was initiated by addition of 25 µl of a CAC1343 protein suspension or whole-cell extracts. The plate was incubated at 37 °C for 60 min (unless indicated otherwise) and the enzyme activity was stopped by the addition of 75 µl of hydroxylamine hydrochloride (2 M, pH 6.5) and incubation at room temperature for 10 min. For final development of ferric acetyl hydroxamate, 50 µl of 15 % (wt/vol) hydroxamate trichloroacetic acid, 4 M HCl, and FeCl<sub>3</sub>·6 H<sub>2</sub>O [5 % (5 % wt/vol) in 0.1 M HCl] were added to each

sample and the color was quantified by absorbance at 505 nm [15]. Samples were compared to acetyl phosphate standards.

### Zymogram assay

A 10-ml culture of *E. coli* BL21 containing pTXB1CAC1343notag was grown in an aerobic shaking incubator at 37 °C. When the culture reached an  $A_{600}$  of approximately 0.5, the culture was split into two 5-ml cultures. One of the cultures was used as a control while the other received 5  $\mu$ l of 1 M IPTG to induce the expression of CAC1343. The cultures were then incubated at 37 °C in a shaking incubator (225 RPM) for 3 h after which the cells were isolated by centrifugation (13,000  $\times$  g) in an Eppendorf 5415D microfuge for 1 min. The supernatant was discarded and the cells were lysed by addition of 150  $\mu$ l Bugbuster Protein Extraction Reagent (Novagen), 0.2  $\mu$ l Benzonase Nuclease (Novagen), 1  $\mu$ l of 200 mM PMSF (Sigma-Aldrich), and 8  $\mu$ l Protease Inhibitor Cocktail (Calbiochem). The tubes were gently mixed on an orbital shaker for 30 min and then centrifuged at 13,000  $\times$  g in an Eppendorf 5415D microfuge for 15 min. The crude cell extract containing supernatant was mixed 1:1 with Native Loading Dye (Bio-Rad) and 10  $\mu$ l of each sample was separated by native electrophoresis in 10 % polyacrylamide gels.

Phosphoketolase zymograms were modified from a transketolase zymogram method described in the Handbook of Detection of Enzymes in Electrophoretic Gels [14]. Staining solution containing 100 mM of Gly–Gly, 0.5 mM of  $\text{NAD}^+$ , 0.16 mM of sodium arsenate, 0.76 mM of ethylenediaminetetraacetic acid, 5 mM of magnesium chloride hexahydrate, 0.6 mM of thiamine pyrophosphate, 24 U/ml of glyceraldehyde-3-phosphate dehydrogenase, and either 0.4 mM of D-xylulose-5-phosphate or 0.4 mM fructose-6-phosphate was used to saturate pieces of filter paper. The filter paper was overlaid onto the gel and care was taken to ensure that there were no air pockets between the filter paper and the gel. The containers were sealed to prevent evaporation of the staining solution and then covered with aluminum foil. After incubation at 37 °C for 1 h, the zymograms were imaged by visualizing NADH fluorescence in a Bio-Rad Versa Doc Imaging System.

### Metabolite analysis

Duplicate cultures of *C. acetobutylicum* were grown in a four-vessel bioreactor as described above except the CGM was supplemented with 0.5 % of glucose, xylose, or arabinose. Then, 10 ml of culture was removed at 1-h intervals for glucose- and arabinose-grown cells and 2-h intervals for xylose-grown cells and placed in a sealed tube

in an ice-water bath for 10 min. The sample was clarified by centrifugation at 5,000  $\times$  g in a Sigma 204 centrifuge equipped with a fixed-angle rotor for 10 min at 4 °C. The supernatant was then filtered through a 0.2- $\mu$ m filter and stored at –80 °C.

HPLC analysis of metabolites was performed on an Agilent 1200 equipped with a refractive index detector and an Aminex HPX-87H cation exchange column (300  $\times$  7.8 mm i.d.  $\times$  9  $\mu$ m) (Bio-Rad) as previously described [3]. Samples (100  $\mu$ l) were injected into the HPLC system and were eluted isocratically with a mobile phase of 3.25 mM  $\text{H}_2\text{SO}_4$  at 0.6 ml/min and 30 °C. Quantification was based on an external calibration curve using pure known components as standards.

## Results

CAC1343 mRNA expression is weakly induced by xylose and strongly induced by arabinose

In a previous report, we used DNA microarrays to show that during acidogenic growth, CAC1343 mRNA was strongly induced by arabinose and slightly induced by xylose when compared to growth on glucose [23]. In that study, CAC1343 was induced 3.9-fold by xylose and 19.4-fold by arabinose (Fig. 1a). DNA microarrays have a limited dynamic range, so quantitative PCR was used to more accurately assess these expression differences. The data (Fig. 1a) showed that when compared to growth on glucose, CAC1343 was induced approximately threefold by xylose and 185-fold by arabinose. Zhang et al. [27] also used quantitative PCR to show that CAC1343 was induced >900-fold during growth on arabinose when compared to growth on glucose in a different medium than was used in the current study. They also reported that CAC1343 is controlled at the transcriptional level by the arabinose regulator AraR [27]. The slight induction of CAC1343 seen during growth on xylose when compared to glucose in the microarray and quantitative PCR experiments is probably due to the loss of catabolite repression or, alternatively, some other unidentified regulatory mechanism. The relatively large induction of CAC1343 during growth on arabinose suggests that the CAC1343 gene product will probably have a greater contribution to the metabolism of arabinose than xylose.

CAC1343 encodes a bi-functional phosphoketolase

To determine if CAC1343 encodes a functional phosphoketolase, CAC1343 was expressed from an IPTG-inducible promoter in *E. coli* and phosphoketolase zymograms were performed on crude cell extracts separated by native

**Fig. 1 a** Gene expression data from microarrays obtained from a previous study and quantitative PCR from the current study showing relative expression of CAC1343 during growth on xylose and arabinose when compared to growth on glucose [23]. The error bars on the qPCR bars show  $\pm$  one standard deviation calculated from three biological replicates. **b** Fructose-6-P and xylulose-5-P zymograms showing phosphoketolase activity of the CAC1343 gene product. Crude cell extracts from *E. coli* strains engineered to express CAC1343 from an IPTG-inducible promoter were separated on a native polyacrylamide gel and stained for phosphoketolase activity as described in the Materials and methods section

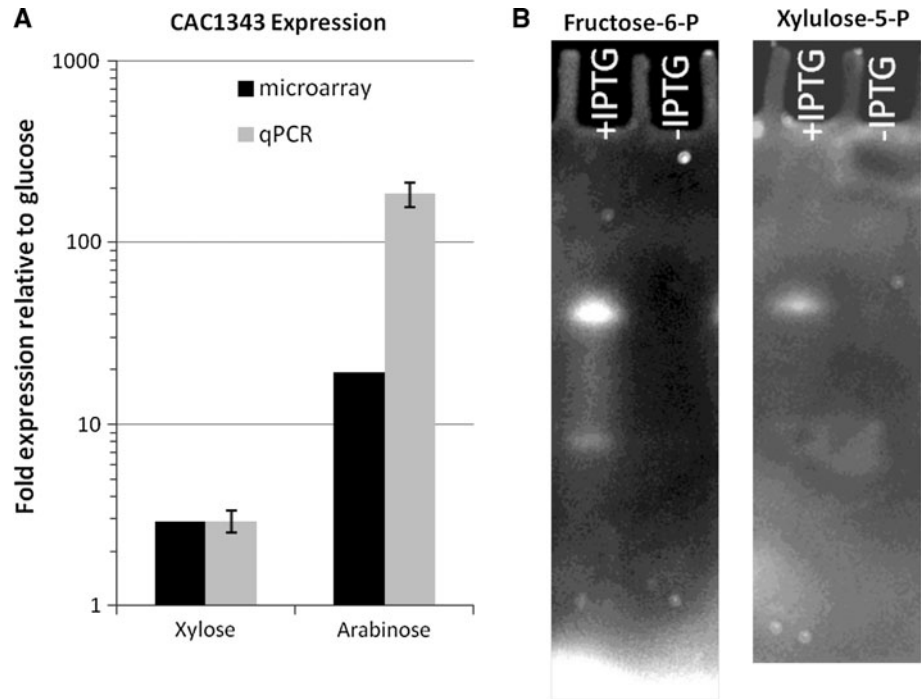


**Table 2** Phosphoketolase-specific activities

|                          | Specific activity (U/mg) |              |
|--------------------------|--------------------------|--------------|
|                          | Fructose-6-P             | Xylulose-5-P |
| Purified recombinant XFP | 6.903                    | 21.348       |
| Crude lysate (arabinose) | 0.096                    | 0.524        |
| Crude lysate (glucose)   | 0.002                    | ND*          |

\* ND Not done

polyacrylamide gel electrophoresis. The results of the zymograms, presented in Fig. 1, indicate CAC1343 expression results in F6P and X5P phosphoketolase activity. Two phosphoketolase bands were present in the F6P zymogram, which may be the result of different oligomerization states of the enzyme. Further enzymatic analysis of the purified phosphoketolase encoded by CAC1343, using the assay developed by Miele et al. [15], indicated that it is thiamine diphosphate-dependent (data not shown) and its specific activities were 6.9 and 21 U/mg for F6P and X5P, respectively (Table 2). To establish whether this activity was present in *C. acetobutylicum* grown on arabinose, whole-cell extracts were tested for phosphoketolase activity using the Miele assay. Negligible activity was seen in extracts of cells propagated on glucose, where as extracts of arabinose-grown cells had activity on F6P and X5P (Table 2) showing that an XFP was induced at the protein level during growth on arabinose. To the best of our knowledge, this is the first demonstration of phosphoketolase activity in a clostridial species. Since CAC1343 encodes a bi-functional xylulose-5-P/fructose-6-P phosphoketolase, we propose the gene

should be named *xfp* to be consistent with phosphoketolase nomenclature used in other organisms.

Arabinose and xylose are metabolized by different pathways

In *C. acetobutylicum*, pentoses were thought to be metabolized via the PPP into the Embden-Meyerhof-Parnas (EMP) pathway intermediates, G3P and F6P (Fig. 2a). During acidogenic growth on a subset of pentoses and hexoses, which are solely metabolized via EMP intermediates, the cell nets 1 ATP, 1 reduced ferredoxin (fdRed) and 1 NADH for every acetyl-CoA that is formed. The cells would gain the most ATP per acetyl-CoA by forming acetate. However, oxidized ferredoxin (fdOx) and NAD<sup>+</sup> need to be regenerated to maintain flux through the EMP and the pyruvate ferredoxin oxidoreductase (PFOR). Reduced ferredoxin is oxidized by the hydrogenase, which allows the cells to use free protons as electron acceptors and results in the formation of H<sub>2</sub>. Additionally, at high FdOx:FdRed ratios, the NADH ferredoxin oxidoreductase can use NADH to reduce ferredoxin, which when coupled with the hydrogenase, allows protons to be used as a sink for electrons from NADH [10]. At low FdOx:FdRed ratios, this reaction is unfavorable, requiring an alternative electron acceptor to oxidize NADH. In *C. acetobutylicum*, acetyl-CoA is used as the alternate electron acceptor by converting it to butyrate, resulting in the formation of one NAD<sup>+</sup> and 1/2 ATP per acetyl-CoA. Table 3 shows the predicted reducing equivalent:acetyl-CoA balance for the

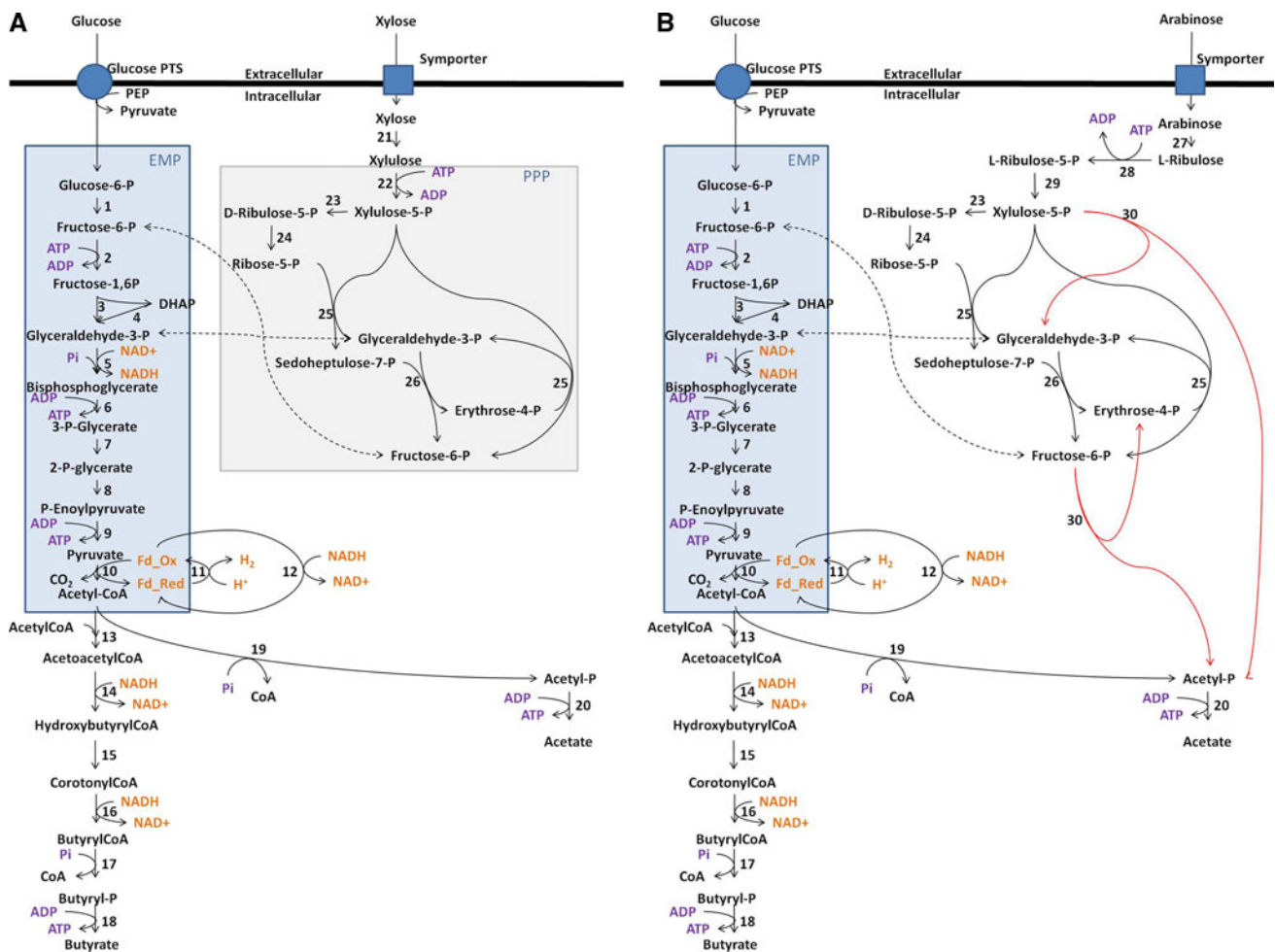


**Fig. 2** Schematic of **a** xylose metabolism via the PPP and **b** arabinose metabolism via the PKP during acidogenic growth. *Arrows* for phosphoketolase reactions are *red*. Enzymes are indicated by *numbers* as follows: 1 phosphoglucose isomerase, 2 phosphofruktokinase, 3 fructose-bis-P aldolase, 4 triosephosphate isomerase, 5 glyceraldehyde-3-P dehydrogenase, 6 phosphoglycerate kinase, 7 phosphoglycerate mutase, 8 enolase, 9 pyruvate kinase, 10 pyruvate ferredoxin

oxidoreductase, 11 hydrogenase, 12  $\text{NAD}^+/\text{NADH}$  oxidoreductase, 13 thiolase, 14 hydroxybutyryl-CoA dehydrogenase, 15 crotonase, 16 butyryl-CoA dehydrogenase, 17 phosphotransbutyrylase, 18 butyrate kinase, 19 phosphotransacetylase, 20 acetate kinase, 21 xylose isomerase, 22 xylulose kinase, 23 epimerase, 24 isomerase, 25 transketolase, 26 transaldolase, 27 arabinose isomerase, 28 ribulose kinase, 29 ribulose-5-P epimerase, 30 phosphoketolase

**Table 3** Predicted metabolic output during metabolism of 30 carbon atoms contained in either five glucoses or six pentoses via the EMP, PPP, and PKP

| Carbohydrate-pathway used | G-3-P formed | Net ATP-EMP | NADH-EMP | Reduced ferredoxin | $\text{CO}_2$ formed | Acetyl-CoA + acetyl-P | Reducing equivalents per acetyl-CoA/P* |
|---------------------------|--------------|-------------|----------|--------------------|----------------------|-----------------------|--|
| 5 glucose-EMP             | 10           | 10          | 10       | 10                 | 10                   | 10                    | 2                                      |
| 6 pentose-PPP             | 10           | 10          | 10       | 10                 | 10                   | 10                    | 2                                      |
| 6 pentose-PKP             | 6            | 6           | 6        | 6                  | 6                    | 12                    | 1                                      |

\* Reducing equivalents are the sum of NADH and reduced ferredoxin

fermentation of 30 carbon atoms, contained in either five glucose molecules or six pentose molecules, to acetyl-CoA via the EMP and the PPP, respectively. According to these calculations, there is no difference in the ATP yield or redox balance during growth on xylose, arabinose, or

glucose, assuming that xylose and arabinose are processed via the PPP. Therefore, if arabinose and xylose are both metabolized via the PPP, the organism would produce similar metabolic outputs (i.e., acetate:butyrate ratios) during acidogenic growth on all three sugars.

In light of the fact that *C. acetobutylicum* induces a bi-functional phosphoketolase during growth on arabinose, an updated view of arabinose metabolism is needed to determine how this enzyme could affect the metabolic output of the cells. Figure 2b shows the predicted pentose phosphoketolase pathway (PKP) for arabinose utilization as it relates to central metabolism. During growth on arabinose, some of the carbon from arabinose will be converted directly to acetyl-P by phosphoketolase activity on either X5P or F6P, avoiding flux through the EMP and complete oxidation of some carbon to CO<sub>2</sub>. Any carbon that fluxes to acetyl-P via the phosphoketolase can be converted to acetate, forming an ATP without the need to regenerate NAD<sup>+</sup> or oxidized ferredoxin. Table 3 shows the predicted reducing equivalent:(acetyl-CoA+ acetyl-P) balance for the fermentation of 30 carbon atoms in six pentose molecules to acetyl-CoA and acetyl-P via the proposed PKP. Formation of six molecules of acetyl-P by the phosphoketolase reduces the number of carbons that will flux through the EMP when compared to PPP metabolism by 12. This equates to the formation of four fewer molecules of G3P, NADH, reduced ferredoxin, ATP, and CO<sub>2</sub>. Carbon is conserved because the cell nets two additional acetyl-P/acetyl-CoA equivalents. A decreased flux through the EMP should increase the FdOx:FdRed ratio allowing more electrons to flow from NADH to the hydrogenase. Overall, the PKP should alleviate some of the need to use acetyl-CoA as an electron acceptor during growth on arabinose. The result should be increased acetate:butyrate production ratios, when compared to sugars metabolized solely via EMP intermediates. In contrast to arabinose, cells grown on xylose weakly induce the phosphoketolase at the transcriptional level, suggesting xylose is probably metabolized primarily via the PPP. If this is the case, then the metabolic output of xylose-fed cells should be similar to that of glucose-fed cells because all of the carbon will be processed by the lower portion of the EMP, as described above.

To determine if the metabolic output of the cells during growth on arabinose and xylose support the predictions made above, we examined the metabolic profiles of *C. acetobutylicum* during acidogenic growth on glucose (EMP control), arabinose, and xylose. The data presented in Fig. 3 show that cells grown on glucose produced a higher concentration of butyrate than acetate, with a final acetate:butyrate ratio of 0.83. A similar trend was seen during growth on xylose, with a final acetate:butyrate ratio of 0.72, suggesting xylose is metabolized via the PPP. In contrast, cells grown on arabinose produced more acetate than butyrate and had a final acetate:butyrate ratio of 1.95, demonstrating that xylose and arabinose are not metabolized by the same pathway. This dramatic shift in metabolic output, combined with transcriptomic data and enzymatic

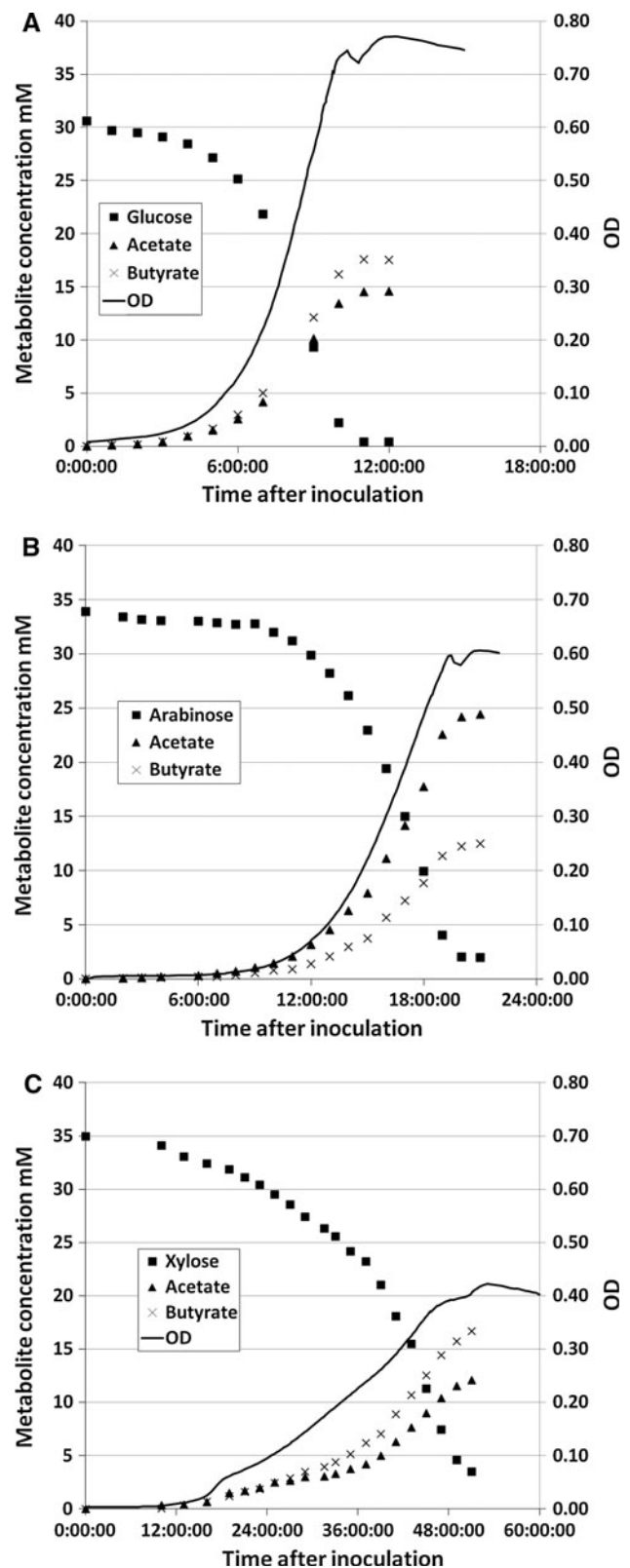


**Fig. 3** Metabolite analysis during growth on **a** glucose, **b** arabinose, and **c** xylose. Data from one of two vessels analyzed for each sugar are shown. Data for the second vessel is available in the supplementary materials

activity, provides strong evidence that arabinose is not processed solely via the PPP in *C. acetobutylicum*. The proposed PKP would result in a shift towards more oxidized products (acetate rather than butyrate). This is consistent with the metabolic output of cells grown on arabinose and indicates that a substantial portion of arabinose is metabolized via the PKP.

## Discussion

*Clostridium acetobutylicum* uses a diverse set of metabolic enzymes to ferment a variety of carbohydrates including pentoses and hexoses. This metabolic diversity makes the organism an ideal candidate for fermentation of waste materials containing heterogeneous carbohydrate mixtures, in which arabinose will be present at physiologically relevant concentrations. In this report, we show *C. acetobutylicum* uses a PKP for arabinose metabolism during acidogenic growth, which resulted in the formation of more oxidized products than would have been formed if the cells had processed arabinose via the PPP. We also show that xylose is probably metabolized via the PPP, suggesting the lack of a functional PKP may contribute to the relatively slow growth rate of the organism on xylose. Here, acidogenic growth was examined but others have shown solvent production during growth on arabinose produces a higher proportion of acetone to butanol when compared to glucose and xylose, suggesting the PKP contributes to metabolism during solvent production [17].

The PKP proposed in this work is similar to the one used by *Lactococcus lactis*, which in a recent report was disrupted, causing the cells to generate a higher proportion of reduced fermentation products [24]. It can be suggested that a deletion in CAC1343 would have a similar effect in *C. acetobutylicum* by shifting metabolism towards butyrate production during growth on arabinose. Additionally, if arabinose is present in mixed carbohydrate substrates, there is the potential that the cells will induce the phosphoketolase that would in turn convert the EMP intermediate F6P to acetyl-P and erythrose-4-P. This would cause a portion of any sugars processed via F6P to flux through the PKP and decrease butyrate production. If this is the case, then deletion of CAC1343 would increase butyrate yields from all arabinose-containing feedstocks, which is a desirable property for biofuel production as butyrate is a precursor for butanol.

Since *C. acetobutylicum* also induces the genes for the PPP during growth on arabinose, it is plausible that some of the arabinose is processed via the PPP. If all of the arabinose was metabolized via the PKP, then the cells would have to generate F6P and glucose-6-P for cell wall biogenesis via gluconeogenesis because the only entry point

into the EMP from the PKP is G3P. These two points, taken together, suggest that the organism likely uses both the PKP and the PPP for arabinose metabolism. The higher activity of XFP on X5P when compared to F6P suggests most carbon fluxes through the PKP via the conversion of X5P to acetyl-P and G3P. If this is the case, then there would be a decreased need for the PPP enzymes transaldolase and transketolase during growth on arabinose when compared to growth on xylose. A clearer difference in the metabolism of xylose and arabinose emerges by combining this information with previous studies. We have shown that there is no difference in mRNA expression levels for transaldolase and transketolase when comparing between growth on xylose and arabinose [23]. Studies by Gu et al. [7] showed increased expression of transaldolase during growth on xylose increases growth rates. The inefficiency of *C. acetobutylicum*'s PPP during growth on arabinose is of little or no consequence, since most carbon is probably not metabolized by transaldolase or transketolase. In contrast, the lack of XFP expression combined with an inefficient PPP during growth on xylose probably causes a backup of the PPP, which can be partially alleviated by increased expression of transaldolase. To gain a better understanding of the role of the PKP in *C. acetobutylicum*, further studies need to be performed to determine the flux of arabinose through the PKP and PPP and the contributions of these pathways to metabolism during solventogenic growth.

## References

1. Albersheim P, Darvill A, Roberts K, Sederoff R, Staehelin A (2011) Plant cell walls. Garland Science, Taylor and Francis Group, LLC, New York, NY
2. Edgar R, Domrachev M, Lash AE (2002) Gene expression omnibus: NCBI gene expression and hybridization array data repository. *Nucleic Acids Res* 30(1):207–210
3. Finch AS, Mackie TD, Sund CJ, Sumner JJ (2011) Metabolite analysis of *Clostridium acetobutylicum*: fermentation in a microbial fuel cell. *Bioresour Technol* 102(1):312–315. doi:10.1016/j.biortech.2010.06.149
4. Gheshlaghi R, Schärer JM, Moo-Young M, Chou CP (2009) Metabolic pathways of clostridia for producing butanol. *Biotechnol Adv* 27(6):764–781. doi:10.1016/j.biotechadv.2009.06.002
5. Goldberg ML, Racker E (1962) Formation and isolation of a glycolaldehyde-phosphoketolase intermediate. *J Biol Chem* 237:3841–3842
6. Grimmler C, Held C, Liebl W, Ehrenreich A (2010) Transcriptional analysis of catabolite repression in *Clostridium acetobutylicum* growing on mixtures of D-glucose and D-xylose. *J Biotechnol* 150(3):315–323. doi:10.1016/j.jbiotec.2010.09.938
7. Gu Y, Li J, Zhang L, Chen J, Niu L, Yang Y, Yang S, Jiang W (2009) Improvement of xylose utilization in *Clostridium acetobutylicum* via expression of the talA gene encoding transaldolase from *Escherichia coli*. *J Biotechnol* 143(4):284–287. doi:10.1016/j.jbiotec.2009.08.009



8. Jones DT, Woods DR (1986) Acetone-butanol fermentation revisited. *Microbiol Rev* 50(4):484–524
9. Jurgens G, Survase S, Berezina O, Sklavounos E, Linnekoski J, Kurkijarvi A, Vakeva M, van Heiningen A, Granstrom T (2012) Butanol production from lignocellulosics. *Biotechnol Lett* 34(8):1415–1434. doi:10.1007/s10529-012-0926-3
10. Kim BH, Gadd GM (2008) *Bacterial physiology and metabolism*. Cambridge University Press, Cambridge
11. Lee J, Yun H, Feist AM, Palsson BO, Lee SY (2008) Genome-scale reconstruction and in silico analysis of the *Clostridium acetobutylicum* ATCC 824 metabolic network. *Appl Microbiol Biot* 80(5):849–862. doi:10.1007/s00253-008-1654-4
12. Lee JY, Jang YS, Lee J, Papoutsakis ET, Lee SY (2009) Metabolic engineering of *Clostridium acetobutylicum* M5 for highly selective butanol production. *Biotechnol J* 4(10):1432–1440. doi:10.1002/biot.200900142
13. Lutke-Eversloh T, Bahl H (2011) Metabolic engineering of *Clostridium acetobutylicum*: recent advances to improve butanol production. *Curr Opin Biotechnol* 22(5):634–647. doi:10.1016/j.copbio.2011.01.011
14. Manchenko GP (2003) *Handbook of detection of enzymes on electrophoretic gels*, 2nd edn. CRC Press, Boca Raton
15. Meile L, Rohr LM, Geissman TA, Herensperger M, Teuber M (2001) Characterization of the D-xylulose 5-phosphate/D-fructose 6-phosphate phosphoketolase gene (xfp) from *Bifidobacterium lactis*. *J Bacteriol* 183(9):2929–2936
16. Nigam PS, Singh A (2011) Production of liquid biofuels from renewable resources. *Prog Energy Combust* 37(1):52–68. doi:10.1016/j.peccs.2010.01.003
17. Ounine K, Petitdemange H, Raval G, Gay R (1983) Acetone-butanol production from pentoses by *Clostridium Acetobutylicum*. *Biotechnol Lett* 5(9):605–610
18. Pfaffl MW (2001) A new mathematical model for relative quantification in real-time RT-PCR. *Nucleic Acids Res* 29(9):e45
19. Ramakers C, Ruijter JM, Deprez RH, Moorman AF (2003) Assumption-free analysis of quantitative real-time polymerase chain reaction (PCR) data. *Neurosci Lett* 339(1):62–66
20. Rozen S, Skaletsky H (2000) Primer3 on the WWW for general users and for biologist programmers. *Methods Mol Biol* 132:365–386
21. Sanchez B, Zuniga M, Gonzalez-Candelas F, de los Reyes-Gavilan CG, Margolles A (2010) Bacterial and eukaryotic phosphoketolases: phylogeny, distribution and evolution. *J Mol Microb Biotech* 18(1):37–51. doi:10.1159/000274310
22. Senger RS, Papoutsakis ET (2008) Genome-scale model for *Clostridium acetobutylicum*: part I. Metabolic network resolution and analysis. *Biotechnol Bioeng* 101 (5):1036–1052. doi:10.1002/bit.22010
23. Servinsky MD, Kiel JT, Dupuy NF, Sund CJ (2010) Transcriptional analysis of differential carbohydrate utilization by *Clostridium acetobutylicum*. *Microbiol-Sgm* 156:3478–3491. doi:10.1099/Mic.0.037085-0
24. Shinkawa S, Okano K, Yoshida S, Tanaka T, Ogino C, Fukuda H, Kondo A (2011) Improved homo l-lactic acid fermentation from xylose by abolishment of the phosphoketolase pathway and enhancement of the pentose phosphate pathway in genetically modified xylose-assimilating *Lactococcus lactis*. *Appl Microbiol Biot* 91(6):1537–1544. doi:10.1007/s00253-011-3342-z
25. Wiesenborn DP, Rudolph FB, Papoutsakis ET (1988) Thiolase from *Clostridium-acetobutylicum* Atcc-824 and its role in the synthesis of acids and solvents. *Appl Environ Microbiol* 54(11):2717–2722
26. Xiao H, Gu Y, Ning Y, Yang Y, Mitchell WJ, Jiang W, Yang S (2011) Confirmation and elimination of xylose metabolism bottlenecks in glucose phosphoenolpyruvate-dependent phosphotransferase system-deficient *Clostridium acetobutylicum* for simultaneous utilization of glucose, xylose, and arabinose. *Appl Environ Microbiol* 77(22):7886–7895. doi:10.1128/AEM.00644-11
27. Zhang L, Leyn SA, Gu Y, Jiang W, Rodionov DA, Yang C (2012) Ribulokinase and transcriptional regulation of arabinose metabolism in *Clostridium acetobutylicum*. *J Bacteriol* 194(5):1055–1064. doi:10.1128/JB.06241-11